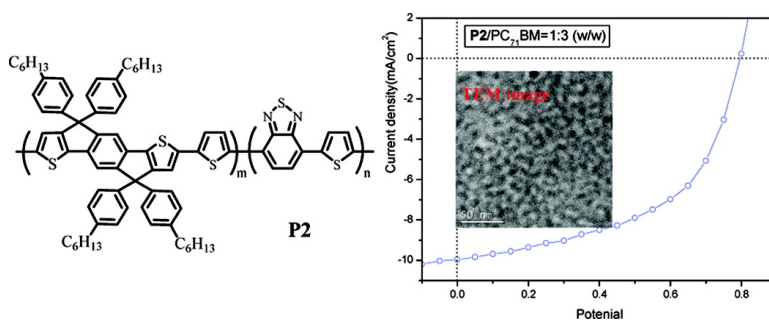


Low-Bandgap Poly(Thiophene-Phenylene-Thiophene) Derivatives with Broadened Absorption Spectra for Use in High-Performance Bulk-Heterojunction Polymer Solar Cells

Chih-Ping Chen, Shu-Hua Chan, Teng-Chih Chao, Ching Ting, and Bao-Tsan Ko

J. Am. Chem. Soc., **2008**, 130 (38), 12828-12833 • DOI: 10.1021/ja801877k • Publication Date (Web): 29 August 2008

Downloaded from <http://pubs.acs.org> on February 8, 2009



More About This Article

Additional resources and features associated with this article are available within the HTML version:

- Supporting Information
- Access to high resolution figures
- Links to articles and content related to this article
- Copyright permission to reproduce figures and/or text from this article

[View the Full Text HTML](#)

Low-Bandgap Poly(Thiophene-Phenylene-Thiophene) Derivatives with Broadened Absorption Spectra for Use in High-Performance Bulk-Heterojunction Polymer Solar Cells

Chih-Ping Chen, Shu-Hua Chan, Teng-Chih Chao, Ching Ting,* and Bao-Tsan Ko*

Materials and Chemical Laboratories, Industrial Technology Research Institute, 195, Sec. 4, Chung Hsing Road, Chutung, Hsinchu, 310, Taiwan

Received March 19, 2008; E-mail: BTKo@itri.org.tw (B.-T.K.); CTing@itri.org.tw (C.T.)

Abstract: Two low-bandgap (LGB) conjugated polymers (**P1** and **P2**) based on thiophene-phenylene-thiophene (TPT) with adequate energy levels have been designed and synthesized for application in bulk-heterojunction polymer solar cells (PSCs). The absorption spectral, electrochemical, field effect hole mobility and photovoltaic properties of LGB TPT derivatives are investigated and compared with poly(3-hexylthiophene) (P3HT). Photophysical studies reveal bandgaps of 1.76 eV for **P1** and 1.70 eV for **P2**, which could effectively harvest broader solar spectrum. In addition, the thin film absorption coefficients of **P1** and **P2** are $1.6 \times 10^5 \text{ cm}^{-1}$ ($\lambda \approx 520 \text{ nm}$) and $1.4 \times 10^5 \text{ cm}^{-1}$ ($\lambda \approx 590 \text{ nm}$), respectively. Electrochemical studies indicate desirable HOMO/LUMO levels that enable a high open circuit voltage while blending them with fullerene derivatives as electron acceptors. Furthermore, both materials show sufficient hole mobility ($3.4 \times 10^{-3} \text{ cm}^2/\text{Vs}$ for **P2**) allowing efficient charge extraction and a good fill-factor for PSC application. High-performance power conversion efficiency (PCE) of 4.4% is obtained under simulated solar light AM 1.5 G (100 mW/cm²) from PSC device with an active layer containing 25 wt% **P2** and 75 wt% [6,6]-phenyl-C71-butyric acid methyl ester (PC₇₁BM), which is superior to that of the analogous P3HT cell (3.9%) under the same experimental condition.

Introduction

Polymer solar cells (PSCs) have attracted strong interest in recent years due to the prospect of low cost, solution-based processing and the capability to fabricate flexible devices.^{1,2} A variety of device compositions have been developed, including polymer/C₆₀,³ polymer/polymer,⁴ and polymer/nanocrystal (NC).⁵ The power conversion efficiency (PCE) of PSCs has been continued to raise and reach 5% under AM 1.5 G^{1,6,7} on the blending thin film composed of poly(3-hexylthiophene) (P3HT) as the donor and [6,6]-phenyl-C61-butyric acid methyl ester (PC₆₁BM) as the acceptor. Although possessing several advantageous properties, P3HT can only absorb part of solar spectrum within the visible region, and thus limits the ultimate performance of device. To improve the PCE of the PSCs, development of new semiconducting polymers with high absorption coefficients and broader solar absorption^{8,9} are of critical importance. For these reasons, low-bandgap (LGB) polymers have been

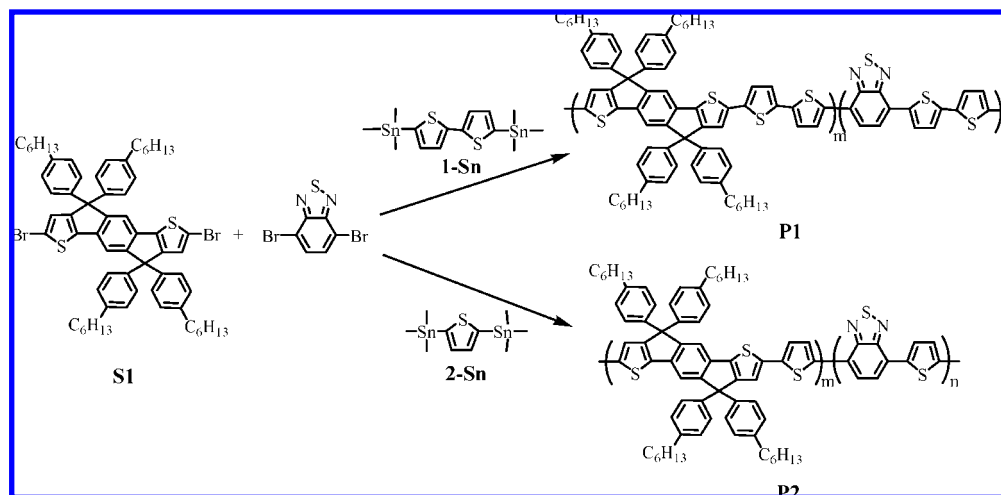
developed to harvest the solar spectrum efficiently in order to generate more photocurrent.^{10–12} Unfortunately, LBG polymers often show better absorption at a long-wavelength range (e.g., Near infrared (NIR)), while some part of visible region absorption are being sacrificed.^{12,13} In addition, besides some recent advances,^{12–14} relatively lower hole mobility and poor solubility are often associated with LBG polymers. The main challenge of LBG polymer engineering is to simultaneously possess high mobility and better utility of sunlight, which have not only narrower bandgaps but also broad absorption bandwidths. The high absorption coefficient and broader absorption could help to improve the harvesting of solar energy, allowing for high photocurrent throughput. Also, the higher charge carrier mobility enables the better carrier transport within active layer without significant photocurrent loss due to the recombination of opposite charges.

In our efforts to design new semiconducting polymers for PSC application, we began with thiophene-phenylene-thiophene

- (1) Kim, J. Y.; Lee, K.; Coates, N. E.; Moses, D.; Nguyen, T.-Q.; Dante, M.; Heeger, A. J. *Science* **2007**, *317*, 222.
- (2) Gunes, S.; Neugebauer, H. S.; Sariciftci, N. S. *Chem. Rev.* **2007**, *107*, 1324.
- (3) Kim, Y.; Cook, S.; Tuladhar, S. M.; Choulis, S. A.; Nelson, J.; Durrant, J. R.; Bradley, D. D. C.; Giles, M.; McCulloch, I.; Ha, C.-S.; Ree, M. *Nat. Mater.* **2006**, *5*, 197.
- (4) Kietzke, T.; Hörhold, H.-H.; Neher, D. *Chem. Mater.* **2005**, *17*, 6532.
- (5) Gur, I.; Fromer, N.; Chen, C. P.; Kanarkas, A.; Alivisatos, A. P. *Nano Lett.* **2007**, *7*, 409.
- (6) Kim, J. Y.; Kim, S. H.; Lee, H.-H.; Lee, K.; Ma, W.; Gong, X.; Heeger, A. J. *Adv. Mater.* **2006**, *18*, 572.
- (7) Kim, K.; Liu, J.; Nambhoosri, M. A. G.; Carroll, D. L. *Appl. Phys. Lett.* **2007**, *90*, 163511.

- (8) Hou, J. H.; Tan, Z. A.; Yan, Y.; He, Y. J.; Yang, C. H.; Li, Y. F. *J. Am. Chem. Soc.* **2006**, *128*, 4911.
- (9) Zhou, E. J.; Tan, Z. A.; Yang, C. H.; Li, Y. F. *Macromol. Rapid Commun.* **2006**, *27*, 793.
- (10) Zhang, F.; Mammo, W.; Andersson, L. M.; Admassie, S.; Andersson, M. R.; Inganäs, O. *Adv. Mater.* **2006**, *18*, 2169.
- (11) Wang, F.; Luo, J.; Yang, K.; Chen, J.; Huang, F.; Cao, Y. *Macromolecules* **2005**, *38*, 2253.
- (12) Blouin, N.; Michaud, A.; Leclerc, M. *Adv. Mater.* **2007**, *19*, 2295.
- (13) Peet, J.; Kim, J. Y.; Coates, N. E.; Ma, W. L.; Moses, D.; Heeger, A. J.; Bazan, G. C. *Nat. Mater.* **2007**, *6*, 497.
- (14) Scharber, M. C.; Mühlbacher, D.; Koppe, M.; Denk, P.; Waldauf, C.; Heeger, A. J.; Brabec, C. J. *Adv. Mater.* **2006**, *18*, 789.

Scheme 1. Synthetic Routes of the TPT-Incorporated LBG Polymers



(TPT) derivatives as the coplanar units.¹⁵ The coplanar chromophores, featuring embedded heteroarens as constituents of coplanar conjugated backbones, may exhibit strong intermolecular π - π interaction, which could enhance degree of π -conjugation and expect to have remarkable hole mobility.¹⁶ The tetra-hexyl-aryl group as peripheral substituents of coplanar backbones tailor intermolecular interactions between polymer chains for better morphologies and processability (**S1**; Scheme 1). In our previous study, the poly(TPT) derivatives possess high field-effect hole mobility (around 10^{-3} cm^2/Vs) which is comparable with P3HT under the same experimental condition. Moreover, while blending with the fullerene acceptors, the promising PSC performance of 3.3% has been achieved.¹⁵ However, the performances of previous poly(TPT)s are limited by the insufficient absorption in the optical property (the bandgap is around 2.1 eV). Accordingly, we present here an extended absorption spectrum of a TPT-based LBG polymer (Scheme 1) for application in bulk-heterojunction photovoltaic cells. The incorporation of 2,1,3-benzothiadiazole (BT) units have been reported to tailor the energy levels of the bandgap (E_g) via donor-acceptor concept.¹⁷ The interaction between alternating electron-rich donors and electron-deficient acceptors will result in a narrower bandgap. These new LBG TPT polymers show high-performance PSC characteristic with 34% increase in photocurrent density (J_{sc}) which can be attributed to have broad and strong absorption band as well as high hole mobility.

Results and Discussion

Polymer Synthesis and Characterization. Recently, we presented the synthesis of **S1** and the poly(TPT) derivatives as PSC materials.¹⁵ The present study further illustrates the introduction of donor-acceptor concept in developing LBG polymers via incorporating BT units. It has been demonstrated that coupling together electron-withdrawing BT units and electron-donating thiophene moieties resulted in a number of existing LBG polymers. However, other than some recent advances,¹²⁻¹⁴ the PSC performances of these polymers are typically lower than

1% due to their poor solubility. In this study, copolymers that consist of 2-(thiophen-2-yl)thiophene (**1**) (or thiophene (**2**)) and **S1** as electron-donating units and BT as electron-accepting moieties were synthesized by Pd(0)-catalyzed Stille coupling polymerization in chlorobenzene under microwave heating conditions (Scheme 1). All of the polymers show good solubility at room temperature in organic solvents such as chloroform (CHCl_3), tetrahydrofuran (THF), and chlorobenzene. The incorporation of tetra-hexyl-substituent on TPT enables them to have good solubility. The molecular structures of the polymers were verified by ^1H NMR and UV-vis spectra. ^1H NMR spectrum of **P2** is shown in Figure 1. The peaks at δ 7.85–8.25 ppm are assigned to the proton resonance of BT unit and the fact that they are shown here as a group of three peaks, indicates the presence of a random copolymer. The characteristic peaks at δ 7.50–7.00 ppm can be assigned to the resonance of protons on the thiophene ring, phenylene ring, and phenyl side groups. There is a peak at δ 2.55 ppm which is attributed to methylene group attached to the phenyl group. The peaks in the ranges of δ 1.60–0.88 ppm arise from tetra-hexyl-substituent of the TPT unit. All of the integral ratios of peak areas between the aromatic and aliphatic signals agree with the corresponding molecular structure of the polymers. The weight-average molecular weight (M_w) and polydispersity index (M_w/M_n) were measured by gel permeation chromatography (GPC) using THF as the eluent and polystyrenes as the internal standards. The M_w of **P1** and **P2** are 26 300 and 38 600, respectively (Table 1). Moreover, the resulting polymers show a good thermal stability (about 5% weight-loss temperature (T_d) above 450 °C) as measured by thermogravimetric analysis (TGA) ($T_d = 460$ °C for **P1** and 510 °C for **P2** sample). The thermal transitions of both polymers were also investigated by differential scanning calorimetry (DSC). However, glass transition temperature (T_g) of **P1** and **P2** were not observed in the range from 40 to 300 °C. The combinations of such good physical properties are highly suitable for PSC application.

Optical Properties. The UV-vis absorption spectra of **P1** and **P2** films are shown in Figure 2, as well as P3HT for comparison. The spectroscopic data of the polymers are summarized in Table 1. **P1** film shows broad π - π^* absorption from 350 to 700 nm and λ_{max} is around 520 nm. The optical bandgap (E_g^{opt}), determined from the onset of absorption of **P1** is 1.76 eV. Compared to our previous report,¹⁵ the strong red shift from

(15) Chan, S.-H.; Chen, C.-P.; Cao, T.-C.; Ting, C.; Ko, B.-T. *Macromolecules* **2008**, *41*, 5519.

(16) Wong, K. T.; Chao, T.-C.; Chi, L.-C.; Chu, Y.-Y.; Balaiah, A.; Chiu, S.-F.; Liu, Y.-H.; Wang, Y. *Org. Lett.* **2006**, *8*, 5033.

(17) van Mulleom, H. A. M.; Vekemans, J. A. J. M.; Havinga, E. E.; Meijer, E. W. *Mater. Sci. Eng., R* **2001**, *32*, 1.

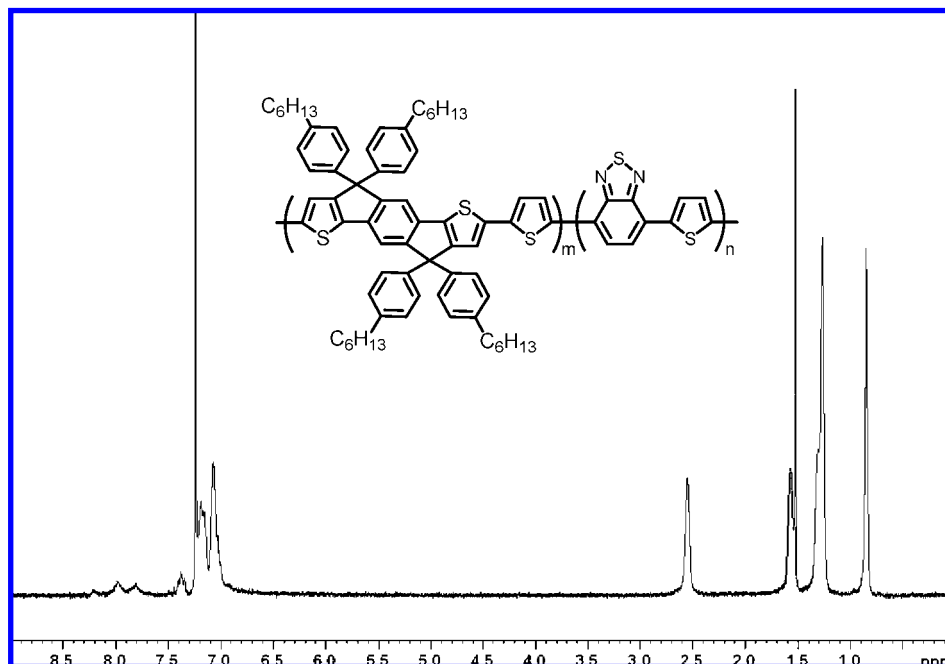


Figure 1. ^1H NMR spectrum and chemical structure of **P2**.

Table 1. Molecular Weights, OTFT Mobility, Optical and Redox Properties of Various Polymers

	M_w (PDI)	λ_{max} (film)	α ($\times 10^5 \text{ cm}^{-1}$)	E_g^{opt} (eV)	E_{ox}^c (V)	HOMO (eV)	LUMO (eV)	μ_{th} (cm^2/Vs)	on/off
P1	26300 (1.55)	520	11^a (1.6) ^b	1.76	1.00	-5.46	-3.56	7.0×10^{-4}	1.3×10^5
P2	38600 (1.74)	590	7.7^a (1.4) ^b	1.70	0.97	-5.43	-3.66	3.4×10^{-3}	5.6×10^6

^a Absorption coefficient was determined at λ_{max} in THF. ^b Absorption coefficient of the solid thin film at λ_{max} . ^c E_{ox} is the onset potential of oxidation of polymer.

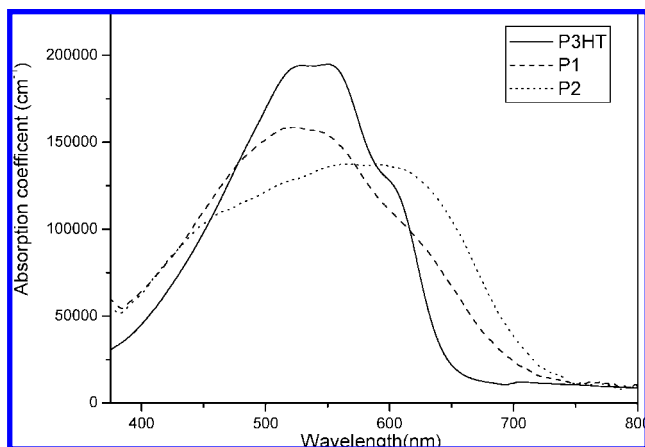


Figure 2. Absorption spectra of poly(TPT)s and P3HT films.

absorption edge from 590 to 700 nm was obtained via introducing the strong electron accepting BT group. Interestingly, **P2** film possesses a broad and strong absorption band in the region from 350 to 730 nm with a λ_{max} at around 590 nm, which shows approximately 20 nm red-shifted compared to that of P3HT. The absorption edge also shows a red shift from 650 (P3HT) to 730 nm, corresponding to a bandgap of 1.70 eV for **P2**. Typically, LBG polymers showed two absorption bands and a transmission valley between them that contributes to lower light harvesting.^{13,14,18} However, **P2** could absorb at a longer

wavelength without diminishing of the shorter wavelength absorption, possibly due to the random copolymer structure of **P2** which combine the absorbance of TPT rich (larger E_g^{opt}) and BT rich (narrower E_g^{opt}) structures.¹⁹ This broad absorption feature should help to improve absorption efficiency of the solar cell performance. Generally, the amount of absorbed light depends not only on the edge of absorption wavelength but also on the intensity of the absorption. Indeed, additional attractive characteristic of **P1** or **P2** is that they have high absorption coefficients that are comparable with P3HT in THF solution. The dilute concentrations (6.6×10^{-3} g/L) of those polymers in THF are conducted to be the same and their absorption coefficient (α) is calculated from Beer's law. As shown in Table 1, **P1** and **P2** have $1.1 \times 10^6 \text{ cm}^{-1}$ at λ_{max} (~ 510 nm) and $7.7 \times 10^5 \text{ cm}^{-1}$ at λ_{max} (~ 570 nm), respectively, which are comparable to that ($\alpha \approx 1.2 \times 10^6 \text{ cm}^{-1}$) of P3HT at its λ_{max} (~ 450 nm). In order to evaluate the absorption property of PSC, the absorption coefficients of solid films are investigated. As depicted in Table 1, the absorption coefficients (α) of the polymer films are measured to be $1.6 \times 10^5 \text{ cm}^{-1}$ at λ_{max} (~ 520 nm) and $1.4 \times 10^5 \text{ cm}^{-1}$ at λ_{max} (~ 590 nm) for **P1** and **P2**, respectively, and $1.9 \times 10^5 \text{ cm}^{-1}$ at λ_{max} (~ 510 nm) for P3HT. Compared to the previous reports,²⁰ the absorption coefficient of P3HT falls in the reasonable range of $1.75\text{--}2.5 \times 10^5 \text{ cm}^{-1}$

(19) Zhu, Z.; Waller, D.; Gaudiana, R.; Morana, M.; Muhlbacher, D.; Scharber, M.; Brabec, C. *Macromolecules* **2007**, *40*, 1981.

(20) (a) Kim, Y.; Cook, S.; Tuladhar, S. M.; Choulis, S. A.; Nelson, J.; Durrant, J. R.; Bradley, D. D. C.; Giles, M.; McCulloch, I.; Ha, C.-S.; Ree, M. *Nat. Mater.* **2006**, *5*, 197. (b) Al-Ibrhim, M.; Roth, H.-K.; Zhokhavets, U.; Gobsch, G.; Sensfuss, S. *Sol. Energy Mater. Sol. Cells* **2005**, *85*, 13.

(18) Chi, C.; Yao, Y.; Yang, Y.; Pei, Q. *J. Am. Chem. Soc.* **2006**, *128*, 8980.

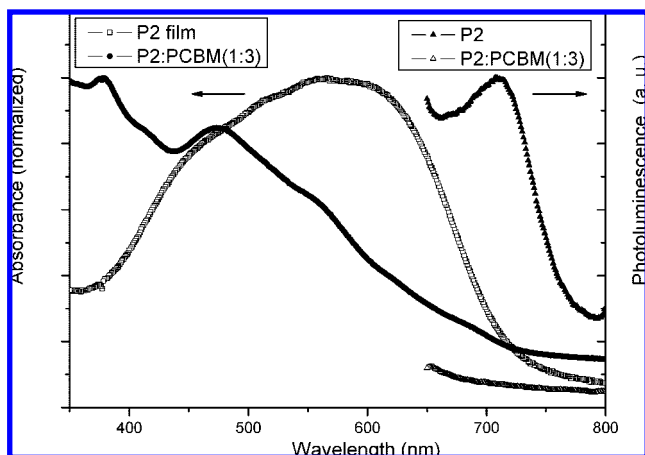


Figure 3. UV-vis spectra of **P2** film (\square), and **P2:PCBM(1:3)** film (\bullet), photoluminescence in **P2** film (\blacktriangle), and photoluminescence quenching for **P2:PCBM(1:3)** (\triangle).

at λ_{\max} . The absorption coefficients at λ_{\max} for **P1** and **P2** are slightly lower than for **P3HT**, but in the same order of magnitude. Besides absorption, photoluminescence (PL) of polymers and their quenching phenomena of the blends are also studied in order to compare their charge transfer efficiencies. The solid film photoluminescence (PL) of the **P2** lie near the red region with an emission maximum at 730 nm and is almost completely quenched by the addition of PCBM by a 1:3 polymer:PCBM weight ratio (Figure 3). The solid film PL of the **P1** shows the same tendency in our experiment. The highly efficient photoluminescence quenching suggests the ultrafast photoinduced charge transfer from the polymer to PCBM.

Electrochemical Properties. The cyclic voltammograms of **P1** and **P2** films on a Pt electrode in acetonitrile solution of 0.1 mol/L Bu_4NPF_6 are summarized in Table 1. The **P1** presents one oxidation process ($E_{\text{ox}} = 1.0$ V) and one reduction process ($E_{\text{red}} = -0.9$ V). From the value of E_{ox} , the highest occupied molecular orbital (HOMO) is calculated according to

$$\text{HOMO} = -(E_{\text{ox}} - E_{1/2}(\text{ferrocene}) + 4.8)\text{V} \quad (1)$$

where E_{ox} is the onset oxidation potential vs SCE. While the lowest unoccupied molecular orbital (LUMO) levels were estimated from the values of E_{red} by

$$\text{LUMO} = -(E_{\text{red}} - E_{1/2}(\text{ferrocene}) + 4.8)\text{V} \quad (2)$$

The HOMO values of **P1** and **P2** were calculated to be -5.46 and -5.43 eV; and the LUMO values of **P1** and **P2** were calculated to be -3.56 and -3.66 eV, accordingly. The electrochemical bandgap (E_{g}^{ec}) was then calculated from the difference between above LUMO and HOMO values. The corresponding E_{g}^{ec} values of **P1** and **P2** are 1.90 and 1.77 eV, which are consistently larger than their $E_{\text{g}}^{\text{opt}}$.⁶ In order to overcome the exciton binding energy of polymer and ensure efficient electron transfer from donor to acceptor, the LUMO energy level of the donor (polymer) must be positioned above the LUMO energy level of the acceptor (PCBM) by at least 0.3 eV. It is worthwhile to compare the energy level diagram of poly(TPT)s with **P3HT** against PCBM, as shown in Figure 4a. The LUMO of poly(TPT)s are ca. 0.6–0.7 eV higher than the LUMO of PCBM, which is well above the required energy for efficient charge separation. In comparison to **P3HT**, the extra beneficial point associated with lower HOMO of the poly(TPT)s

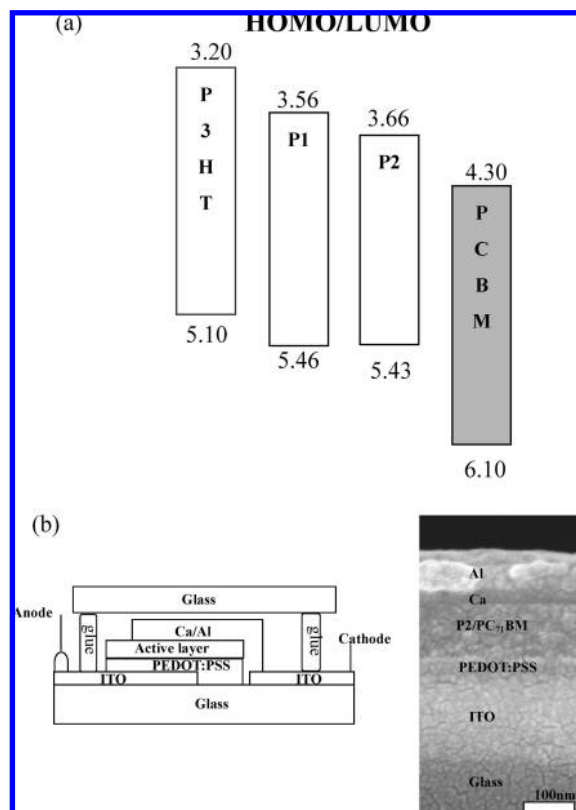


Figure 4. (a) Energy-level diagram showing the HOMO and LUMO energy levels of **P1**, **P2**, **P3HT**, and PCBM. (b) The device architecture (left) and SEM cross-sectional image (right) of the PSC. Scale bars, 100 nm. ITO, indium tin oxide.

is the advantage of higher open circuit voltage (V_{oc}) of photovoltaic devices.

Hole Mobility from Field Effect Transistor Characteristics. High charge-carrier mobility is an essential property to ensure efficient charge extraction. To diminish photocurrent loss in PSCs, a carrier mobility of $>10^{-3}$ cm^2/Vs is necessary for high performance PSC devices.¹⁹ The field-effect carrier mobility of the coplanar conjugated copolymers were investigated by thin film field-effect transistors (FETs) according to our previous work.¹⁵ The source-drain current (I_{DS}) as a function of source-drain voltage (V_{DS}) at different gate voltages (V_{G}) from 0 to -40 V was utilized. Transistor behavior was observed via applying negative V_{G} , indicating that the fabricated FET had p-channel characteristics. The field-effect hole mobility (μ) was estimated from the saturation regime current of I_{DS} approaches by

$$I_{\text{D}} = (W/2L)C_0\mu(V_{\text{G}} - V_{\text{T}})^2 \quad (3)$$

where W is the channel width (1000 μm), L is the channel length (10 μm), C_0 is the capacitance per unit area of the gate dielectric layer (SiO_2 , 100 nm, $C_0 = 34.5$ nF/cm^2), and V_{T} is the threshold voltage. The hole mobility of poly(TPT)s was thus calculated from the transfer characteristics of the OFETs involving plotting $I_{\text{D}}^{1/2}$ vs V_{G} and was summarized in Table 1. A field-effect hole mobility of 7.0×10^{-4} cm^2/Vs and an on/off ratio of 1.3×10^5 were observed in **P1** FETs. An even more improved hole mobility of 3.4×10^{-3} cm^2/Vs and better on/off ratio (5.6×10^6) were obtained for **P2**. The mobility of **P3HT** is about 5.6×10^{-2} cm^2/Vs and an on/off ratio of 1.3×10^3 under the same experimental condition. The hole mobility is within the desirable

Table 2. Characteristic Current-Voltage Parameters from Device Testing at Standard AM 1.5G Conditions

	polymer/PCBM(w/w ratio)	J_{sc} (mA/cm ²)	V_{oc} (V)	FF	η (%) ^d
P3HT ^a	1:1 ^b	9.9	0.64	0.62	3.9
P3HT ^a	1:1 ^c	7.7	0.65	0.68	3.4
P1	1:3 ^b	5.4	0.80	0.47	2.0
P1	1:3 ^c	8.7	0.84	0.53	3.9
P2	1:3 ^b	6.2	0.80	0.51	2.5
P2	1:3 ^c	10.1	0.80	0.53	4.3

^a Purchased from Rieke-Metal (4002E series). ^b Using PC₆₁BM (Purchased from Nano-C) as acceptors. ^c Using PC₇₁BM (Purchased from Solenne) as acceptors. ^d The average value of power conversion efficiency is calculated from 4 pixels in the PSC device.

range for PSC material allowing efficient charge extraction and a good fill factor.

Photovoltaic Properties. The photovoltaic cells were fabricated by spin-coating blend film from a dichlorobenzene (DCB) solution of PCBM/Polymer. Thin-film solar cells (glass/ITO/PEDOT:PSS/Polymer:PCBM/Ca/Al; PEDOT:PSS:Poly(3, 4-ethylenedioxythiophene): poly(styrenesulfonate)) were fabricated using method similar to previous reports.^{5,15} The active layers of poly(TPT) devices were fabricated without annealing process. After encapsulation, the I–V characteristic was measured in air. Figure 4b shows the structure and the SEM image of a typical PSC cell. Cross-sectional SEM image of the device shows clear individual layers without interlayer mixing. The thickness of ITO, PEDOT:PSS, Ca and Al are 190, 30, 30, and 80 nm, respectively. The thickness of active layer can be controlled by changing the spin-coated rate and the concentration of active layer solution. The optimal performances of poly(TPT)s were obtained from conditions of a 7.5 mg/mL DCB solution, 500 rpm of spin-coated rate for 30 s, and polymers/PCBM ratio of 1:3 (w/w). The thickness of active layer is about 90 nm from SEM image. In our case, the lower content of PCBM (<67 wt%) leads to inefficient of electron–hole separation and nonsuitable morphology. With increasing PCBM content, both the J_{sc} and FF increase for poly(TPT)s devices. Further increasing PCBM from 1:3 to 1:4 (w/w), both the J_{sc} and FF are decreased (see Supporting Information). Data in Table 2 summarize the output characteristics of the **P1**, **P2**, and P3HT devices. The cell performance of P3HT is comparable with the earlier literature results, with the optimum efficiency being around 3.9%, while prepared from a 17 mg/mL (P3HT:PC₆₁BM = 1:1 (w/w)) DCB solution. For the devices based on poly(TPT), up to 75 wt.% of PCBM is required for optimal performance. It has also been demonstrated in previous study that improved light absorption can be achieved by using PC₇₁BM blended with MDMO-PPV,²¹ resulting in 50% higher short circuit current density (J_{sc}) and the best efficiency. Our study also shows that a higher efficiencies of poly(TPT) devices can be obtained while PC₇₁BM is used instead of PC₆₁BM as depicted in Table 2. The significantly higher short-circuit current density observed is likely attributed to the considerably higher absorption of PC₇₁BM in the visible region. The effect becomes particularly significant when high content of PCBM (~75%) is used. For the purpose of direct comparison, the P3HT/PC₇₁BM device was also fabricated, and an efficiency of approximately 3.4% could be achieved. The I–V characteristic of a representative cell prepared from **P1** or **P2** blend with PC₇₁BM is shown in

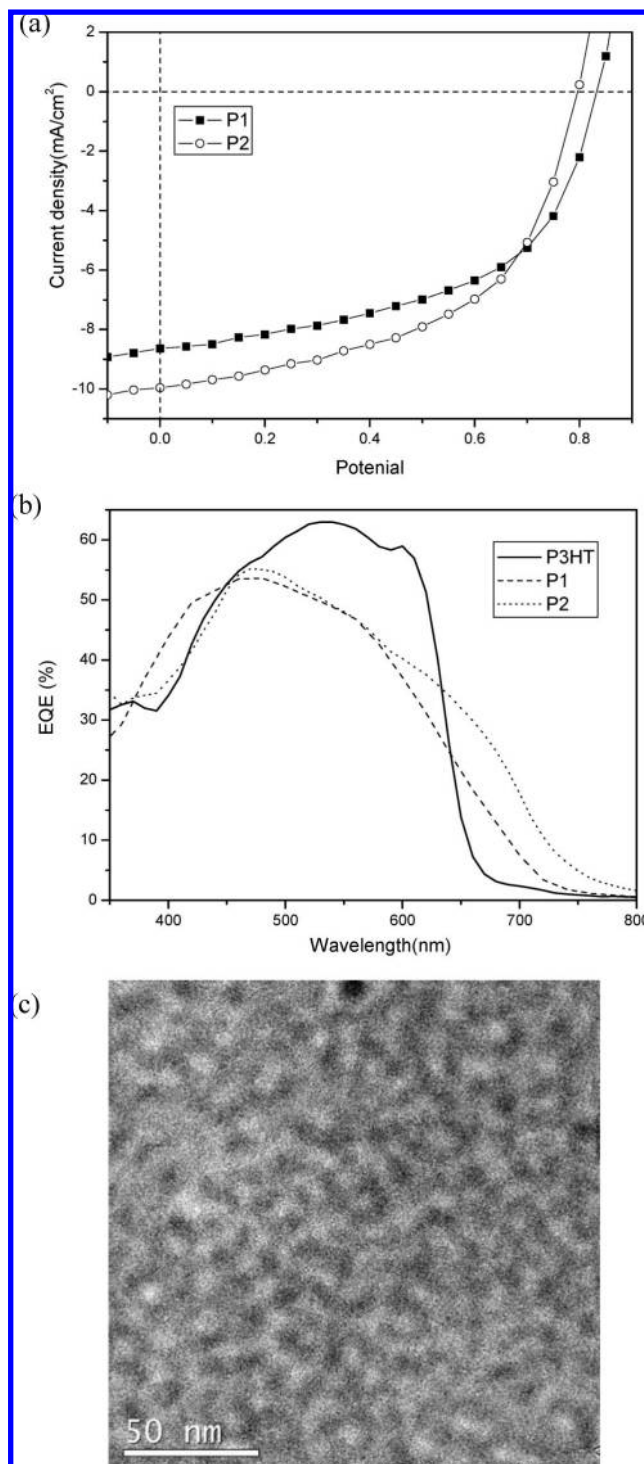


Figure 5. (a) Current density-potential characteristics of **P1** and **P2** solar cell devices under illumination with AM 1.5G solar simulated light (100 mW/cm²) (**P1**(■) and **P2**(○)). (b) The external quantum efficiency (EQE) spectra of devices fabricated with **P3HT**/PC₆₁BM and poly(**TPT**)/PC₇₁BM system. (c) Transmission electron micrographs of **P2**/PC₇₁BM (1:3) thin film. (The scale bar is 50nm).

Figure 5a. The **P2** cell has highest AM1.5G power conversion efficiency (PCE) of 4.4%, with a short circuit current density (J_{sc}) of 10.2 mA/cm², an open circuit voltage (V_{oc}) of 0.81 V, and a fill factor (FF) of 0.53. The PCE of **P2** sample is reproducible and the values are from 4.1 to 4.3% from 5 individual PSC devices. This performance represents one of the highest values among known LBG polymers. In comparison

(21) Wienk, M. M.; Kroon, J. M.; Verhees, W. J. H.; Knol, J.; Hummelen, J. C.; van Hal, P. A.; Janssen, R. A. J. *Angew. Chem., Int. Ed.* **2003**, *42*, 3371.

with the device based on P3HT, the open circuit voltage of the devices based on the TPT polymers increases by ca. 0.16 V. The overall PCE is slightly higher than the corresponding P3HT device. Generally, V_{oc} is related to the difference between HOMO of donor (polymer) and LUMO of acceptor (PCBM).¹⁸ The higher V_{oc} is consistent with the lower HOMO energy levels of the **P2** (Figure 4a). The PCE of **P1** device is lower in comparison with **P2** device, which is due primarily to a remarkable decrease in current density as V_{oc} and FF are comparable. The lower J_{sc} associated with **P1** could be explained by the difference in UV-vis spectra of **P1** and **P2**. Apparently, visible light is more efficiently absorbed by **P2** due to its lower bandgap property. Figure 5(b) compares the external quantum efficiency (EQE) spectra of devices fabricated with P3HT/PC₆₁BM and poly(TPT)/PC₇₁BM materials. The P3HT device shows the typical spectral response with a maximum EQE of 63% at 540 nm, similar to the previous studies.^{8,22} The spectral response of the **P2** device reveals a significant contribution of EQE in the wavelength between 350 and 750 nm and is consistent with UV-vis spectrum of **P2**/PC₇₁BM blend film (Figure 3) with the maximum EQE being approximately 55% at 470 nm. Convolution of the spectral response with the photon flux AM 1.5G spectrum (100 mW/cm²) gives an estimate for the J_{sc} under irradiation. The calculated J_{sc} values for P3HT, **P1**, and **P2** devices are 8.8, 7.8, and 8.6 mA/cm², respectively. Due to the mismatch between EQE and photon flux AM 1.5, there are approximately 10% mismatch between convolution and solar simulator data.

The morphological requirement for the active layer in high performance PSCs is nanophase separation, which enables large interface area for exciton dissociation and, in the mean times, continuous percolating path for hole and electron transport to the corresponding electrodes.²³ Figure 5b shows transmission electron microscopy (TEM) image of **P2**/PC₇₁BM blend film. The main morphological feature of the composite film shows a homogeneous distribution of the two components within the nanoscale. The dark areas are attributed to PCBM domains because the electron scattering density of PCBM is higher than that of conjugated polymer.²⁴ The PCBM domains are around 10 nm and homogeneously distributed in the matrix. The bright patterns of **P2** domains show interpenetrating network allowing better percolating of holes carrier. Accordingly, the nanoscale phase separation between electron donor and acceptor materials allowing large areas of interface for better photogenerated charges and desirable J_{sc} . However, the possibility of recombination of hole and electron carriers at these high interfacial areas could also be enhanced. This might be the reason why the FF values of poly(TPT)s devices has not reached its utmost value. Indeed, PSC performance is known to have strong correlation of active layer morphology, the proper organization of polymers and fullerenes will help to achieve the optimum performance. Further work in identifying this correlation

between the morphological properties and device performance is undergoing.

To be viable in the commercial application, PSC devices should not only offer high efficiencies and low cost but also lifetimes (50% degradation) of at least 10 000 h.²⁵ Generally, PSC devices show only moderate stability when encapsulated rigorously.²⁶ The low work function cathode metals, such as Al and Ca, rapidly undergo oxidation when exposed to air and will significantly decrease the performance. Even in an inert atmosphere (in a glovebox), some degradation is usually observed already within a few hours of operation. Except for being sensitive to oxygen, moisture, or UV radiation, the other limitation of the stability of PSCs comes from the possible morphologic instability of the photoactive layer. For instance, the demixing and diffusion between interface of different layers and polymer/fullerene domains will accelerate degradation. In our preliminary work, the stability of the devices is demonstrated under dark/air condition after encapsulation by using UV-curing glue. After 1500 h, the efficiency decreased from 4.1 to 3.5% (see Supporting Information). The device shows only 15% loss after 2 months storage in air confirms the good stability of the poly(TPT) PSC devices. The accelerated life testing (ALT) is underway to evaluate the reliability and the degradation mechanism of poly(TPT) devices.

Conclusions

Low-bandgap conjugated polymers containing electron-donating thiophene-phenylene-thiophene (TPT) units and electron-accepting 2,1,3-benzothiadiazole moieties have been synthesized. Copolymers that consist of 2-(thiophen-2-yl)thiophene (**1**) (or thiophene (**2**)) and **S1** as electron-donating units and BT as electron-accepting moieties were obtained by Stille coupling polymerization. The absorption spectral, electrochemical, and photovoltaic properties of **P1** and **P2** suggest them to be the potential candidates of next generation solar cell materials. Photovoltaic cells based on these polymer blends with PC₇₁BM have a highest power conversion efficiency of 4.4%. The combination of this electron-donating group and various electron-accepting units could lead to manifold low bandgap polymers for application in photovoltaic science. Design and synthesis of different LBG semiconducting polymers containing TPT units are underway, includes choices of other acceptor monomers and controlling the bandgap to achieve NIR absorption.

Acknowledgment. The authors would like to thank the Ministry of Economic Affairs, Taiwan, for financially supporting this research.

Supporting Information Available: Experimental details of the synthesis and characteristic of the polymers, the detail fabrication and characterization of the PSC devices and instruments. This material is available free of charge via the Internet at <http://pubs.acs.org>.

JA801877K

- (22) Li, G.; Shrotriya, V.; Huang, J.; Yao, Y.; Tommoriarty; Emery, K.; Yang, Y. *Nat. Mater.* **2005**, *4*, 864.
(23) Yang, X.; Loos, J. *Macromolecules* **2007**, *40*, 1354.
(24) Yang, X.; van Duren, J. K. J.; Janssen, R. A. J.; Michels, M. A. J.; Loos, J. *Macromolecules* **2004**, *37*, 2151.

- (25) Brabec, C. J. *Sol. Energy Mater. Sol. Cells* **2004**, *83*, 273.
(26) Dennler, G.; Lungenschmied, C.; Neugebauer, H.; Sariciftci, N. S.; Latreche, M.; Czeremuszkin, G.; Wertheimer, M. R. *Thin Solid Films* **2006**, *511*, 349.